Journal of Marine Research, 63, 901–929, 2005

Two coastal upwelling domains in the northern California Current system

by Adriana Huyer[1,2], Jane H. Fleischbein[1], Julie Keister[1], P. Michael Kosro[1], Natalie Perlin[1], Robert L. Smith[1] and Patricia A. Wheeler[1]

ABSTRACT

A pair of hydrographic sections, one north and one south of Cape Blanco at 42.9N, was sampled in five summers (1998–2000 and 2002–2003). The NH line at 44.6N lies about 130 km south of the Columbia River, and spans a relatively wide shelf off Newport, Oregon. The CR line at 41.9N off Crescent City, California, lies 300 km farther south and spans a narrower shelf. Summer winds are predominantly southward in both locations but the southward winds are stronger on the CR line. Sampling included CTD/rosette casts (to measure temperature, salinity, dissolved oxygen, nutrients, chlorophyll), zooplankton net tows and continuous operation of an Acoustic Doppler Current Profiler. We summarize and compare July-August observations from the two locations. We find significant summer-season differences in the coastal upwelling domains north and south of Cape Blanco. Compared to the domain off Newport, the domain off Crescent City has a more saline, cooler, denser and thicker surface mixed layer, a wider coastal zone inshore of the upwelling front and jet, higher nutrient concentrations in the photic zone and higher phytoplankton biomass. The southward coastal jet lies near the coast (about 20–30 km offshore, over the shelf) on the NH line, but far from shore (about 120 km) on the CR line; a weak secondary jet lies near the shelf-break (35 km from shore) off Crescent City. Phytoplankton tend to be light-limited on the CR line and nutrient-limited on the NH line. Copepod biomass is high (15 mg C m^{-3}) inshore of the mid-shelf on both NH and CR lines, and is also high in the core of the coastal jet off Crescent City. The CR line shows evidence of deep chlorophyll pockets that have been subducted from the surface layer. We attribute these significant differences to stronger mean southward wind stress over the southern domain, to strong small-scale wind stress curl in the lee of Cape Blanco, and to the reduced influence of the Columbia River discharge in this region.

1. Introduction

For many years, there has been evidence that Cape Blanco on the Oregon coast (Fig. 1) marks an important divide in the northern California Current system, particularly during the upwelling season (e.g., Parrish *et al*., 1981). Although most studies of the Oregon coastal upwelling regime were situated north of Cape Blanco, there were strong indications that the upwelling domain south of Cape Blanco differs in summer from the one off central Oregon in many respects: prevailing wind stress (Fig. 2), alongshore currents (Smith,

1. College of Oceanic and Atmospheric Sciences, Oregon State University, 104 COAS Admin Building, Corvallis, Oregon, 97331-5003, U.S.A.
2. Corresponding author. ***email: ahuyer@coas.oregonstate.edu***

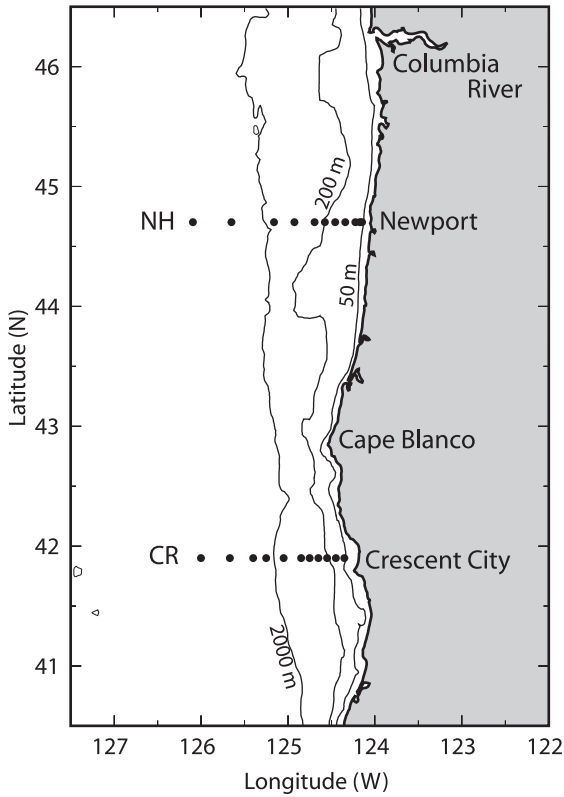

Figure 1. Shelf and coastline geometry in the study region, showing the standard CTD stations of each section, the location of Cape Blanco, Columbia River estuary, and the 50, 200 and 2000 m isobaths.

1995), temperature, salinity, nutrients, phytoplankton, zooplankton and even salmon (Weitkamp *et al.*, 1997). The recent U. S. GLOBEC NorthEast Pacific Program made a systematic effort to quantify these differences through a six-year program of repeated hydrographic surveys (Fig. 1). Results from that program are used here to compare these two domains during the July-August peak of the summer upwelling season (Fig. 2).

The early studies of Oregon coastal upwelling were concentrated in a region of relatively simple topography between 44.5 and 45.5N near Newport, Oregon, about 130 km south of the Columbia River estuary. In this region, the upwelling front generally lies inshore of the shelf-break (Mooers *et al.*, 1976). The baroclinic coastal jet flows equatorward along the mid-shelf and current fluctuations tend to be aligned with isobaths (Kundu and Allen, 1976). The cross-shelf circulation tends to be nearly two-dimensional and in reasonable agreement with the Ekman transport estimated from the wind (Smith, 1981). Surface waters are usually much colder and saltier over the inner shelf than over the shelf-break (Halpern, 1976), and peak chlorophyll concentrations tend to occur over the inner half of continental shelf (Small and Menzies, 1981).

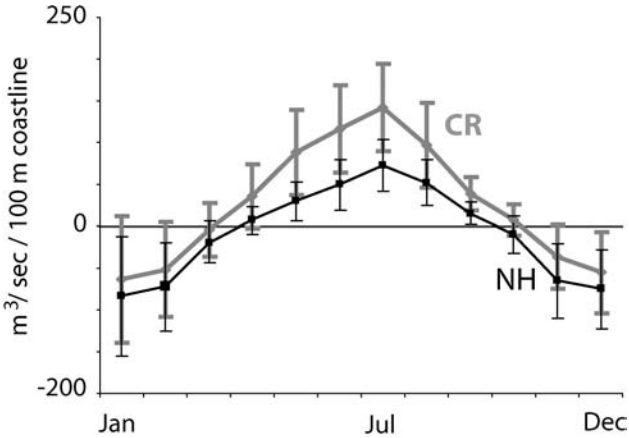

Figure 2. Long-term (1967–1991) monthly means (±1 standard deviation) of the coastal upwelling index at 45N, 125W (black) and 42N, 125W (gray). The index is proportional to the alongshore (southward) component of the local wind stress calculated from large-scale pressure fields. (Data provided by Pacific Environmental Group, www.pfeg.noaa.gov).

A few early studies were conducted near the Oregon border at 42N, south of Cape Blanco, in a region where the continental shelf is rugged and narrow. Smith *et al.* (1966) estimated the cross-shelf and vertical transport from a hydrographic section at 42N that was sampled twice in three days early in the upwelling season (May 1963), and they found reasonable agreement with Ekman transport estimated from wind data. In August 1962, the upwelling front lay more than 60 km offshore at 42N (Laurs, 1967); surface salinity and nutrient concentrations were observed to be as high over the shelf-break as over the inner shelf. An August 1963 survey of the region between Cape Blanco and the Oregon border (Laurs, 1967) shows a salinity front and associated baroclinic jet turning offshore at about 42.5N, 125.2W; the upwelling front already lay offshore of the shelf-break at 42.8N, directly west of Cape Blanco. More recent studies, which include satellite images of sea-surface temperature, drifters and acoustic profiling current surveys, show the seasonal development of coastal upwelling (Smith, 1995; Barth and Smith, 1998; Barth *et al*., 2000; 2005). These studies indicate that the coastal upwelling front and jet follow the shelf topography early in the upwelling season but by mid-summer (July-August) meander around Heceta Bank (near 44N) and around Cape Blanco (near 43N) where they veer far offshore. Observations (Barth *et al.*, 2005) show that the jet near 42N moved about 80 km seaward from the shelf-break between early June and early August. A recent dynamical model for the region (Gan *et al*., 2005) captures many of the jet's features except the extent of its offshore displacement.

Determining whether the differences between the upwelling ecosystems north and south of Cape Blanco are statistically significant was one of the central goals of the U.S. GLOBEC North East Pacific Program's Long Term Observation Program in the California Current. To address this goal, a pair of hydrographic sections, one north and one south of

Cape Blanco (Fig. 1), was sampled in five summers (1998–2000 and 2002–2003); our attempt to sample both sections in a sixth summer (2001) was frustrated by breakdown of the ship's propulsion system. These observations were made after El Niño of 1997–8 which significantly perturbed the marine ecosystem in this region (Huyer *et al*., 2002; Corwith and Wheeler, 2002; Kosro, 2002; Peterson and Keister, 2002); the major effects of El Niño were gone from the region by the time of the first summer survey (August 1998). In this paper, we summarize the 1998–2003 summer observations, compare and contrast results from the two locations, and discuss probable causes of the major differences between the two domains.

2. Methods: Sampling along paired hydrographic sections

The NH line at 44.6N off Newport, Oregon, lies about 130 km south of the mouth of the Columbia River, and spans a relatively wide shelf; this line was sampled regularly (at least seasonally) from 1961 to 1971 and then sporadically until the present study (Smith *et al.*, 2001). The CR line at 41.9N off Crescent City, California, lies 300 km farther south and spans a narrower shelf; this line was originally sampled during the 1981–1984 SuperCODE experiment (Huyer *et al.*, 2002). The winds were southward at both locations around the time of our summer cruises but the southward winds are stronger off Crescent City than off Newport (Fig. 3). Satellite images of sea-surface temperature for each summer survey cruise (Fig. 4) confirm the earlier impression that the front between cool inshore waters and warm offshore waters lies nearer shore off Newport than off Crescent City in summer, and that there tend to be fewer frontal meanders or eddies near Newport than near Crescent City.

The NH line consists of 12 CTD stations whose separation increases with distance from shore; the most offshore station, NH-85, is at 126.05W, 157 km from shore. The CR line originally consisted of nine CTD stations with the most offshore at 125.3W. This section was extended in 2000 by adding two stations (at 125.7W and 126.0W). In 2002 and 2003, the station CR-9 at 125.3W was dropped in favor of CR-9a at 125.4W. Rosette sampling for biochemical properties was made at selected stations (9, 28, 46, 65, 84, 120, 157 km off Newport; 8, 23, 31, 41, 66, 100, and 147 km off Crescent City); zooplankton net tows were made at most of these locations and at additional shelf stations 18 km off Newport and 16 km off Crescent City. A shipborne Acoustic Doppler Current Profiler was operated continuously along each section.

CTD casts typically penetrated at least 90% of the water column over the outer continental shelf and upper slope, and sampled to within 5 m of the bottom over the inner shelf; the maximum sampling depth was 1000 m. The SeaBird Electronics *9/11 plus* CTD was equipped with dual ducted temperature and conductivity sensors, a Digiquartz pressure sensor, and a dissolved oxygen sensor (except in 1998). *In situ* calibration samples were collected for salinity (2–3 samples at each station) and for oxygen (10–12 samples at each of 3–5 stations per cruise). Details of CTD data collection, calibration and processing are available in a series of data reports (Fleischbein *et al.*, 1999; 2001; 2002; 2003). Accuracy of the processed data is estimated to be better than ± 0.01°C for temperature,

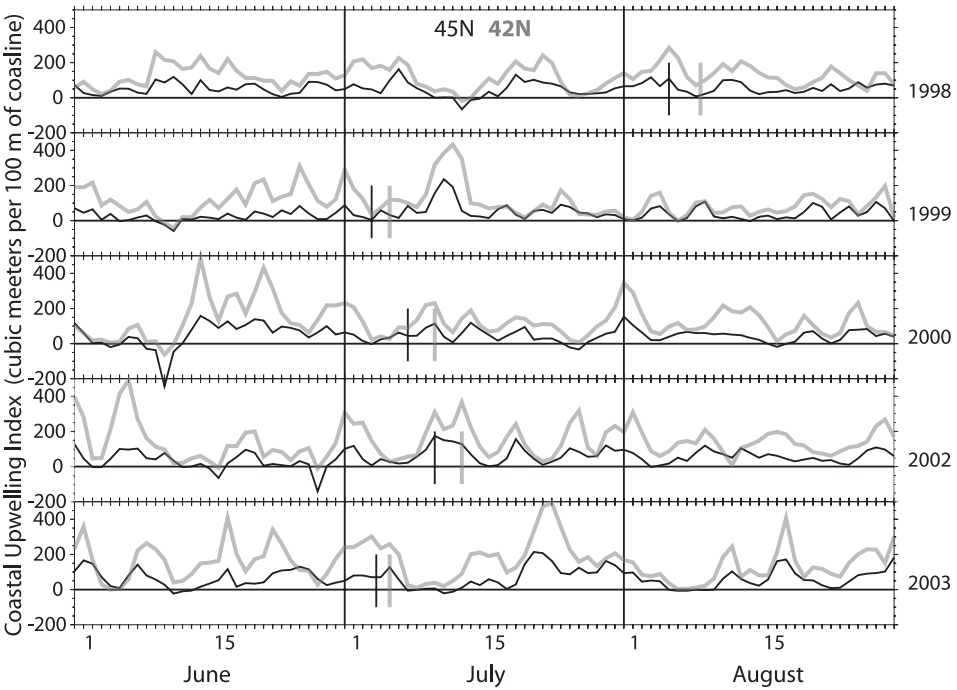

Figure 3. Daily values of the coastal upwelling index at 45N, 125W (black) and 42N, 125W (gray) in summer (June 1 through August 31) of 1998, 1999, 2000, 2002 and 2003 (provided by Pacific Environmental Group). The average value for each month is within one standard deviation of the corresponding long-term monthly means shown in Figure 2. Short vertical lines indicate dates of hydrographic sampling on the NH-line (black) and CR-line (gray).

$\pm$0.003 psu for salinity, $\pm$1 dbar for pressure, and $\pm$0.2 ml/l for dissolved oxygen. The CTD package included a fluorometer on each cruise. In 2002 and 2003, the package also included a Biospherical Instruments QSP200L optical sensor to measure the photosynthetically available radiation (PAR, 400–700 nanometers).

Chemical and biological sampling was conducted at most stations. Water samples from the upper 150 m were analyzed to determine concentrations of inorganic nutrients (nitrate, phosphate, silicate, nitrite, ammonium), phytoplankton biomass (chlorophyll-*a*), particulate organic carbon (POC) and nitrogen (PON), and dissolved organic carbon (DOC) and nitrogen (DON). Samples were collected with 5-liter Niskin bottles on a 12-bottle rosette, with samples taken at about 150 m, 100 m, and at 10 m intervals in the upper 70 m. Analytical methods have been described by Corwith and Wheeler (2002) and by Hill and Wheeler (2002).

Zooplankton samples were collected at many stations using a 0.5 m diameter, 202 μm mesh net towed vertically to the surface at a rate of 30 m min^{-1} from a maximum depth of 100 m (from about 5 m of the bottom in shallower water). A TSK flowmeter was used to monitor the amount of water filtered. The samples were preserved in 5% buffered

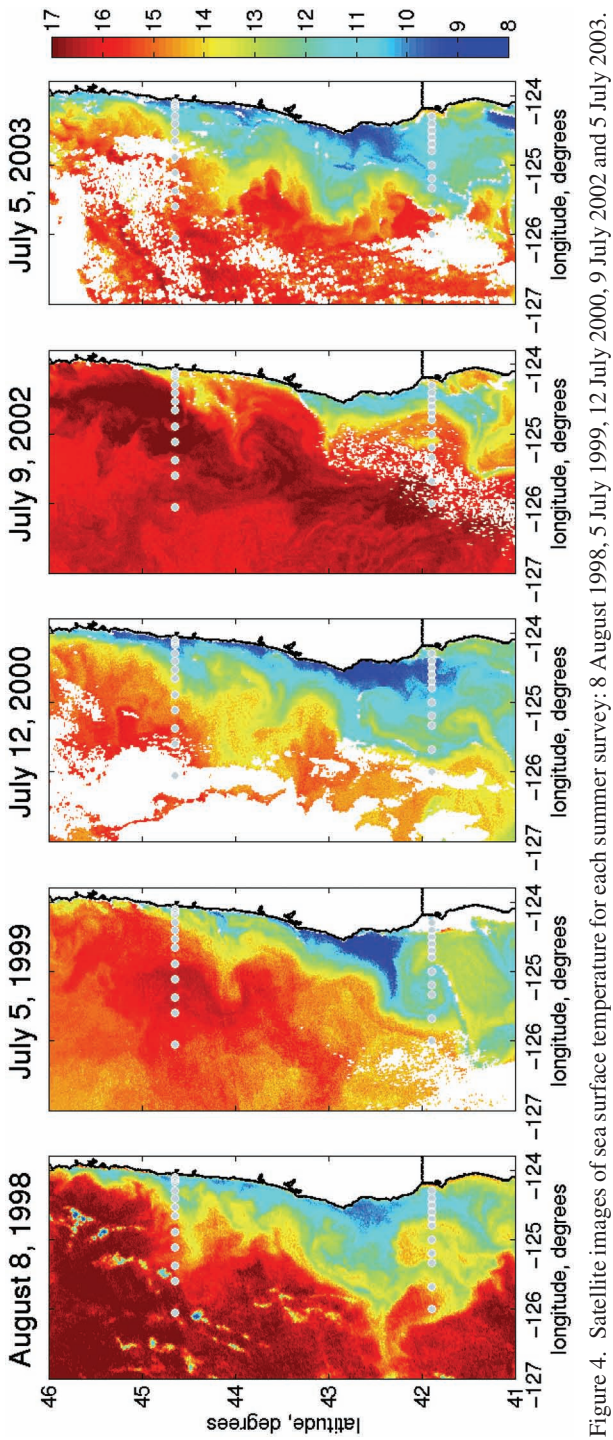

Figure 4. Satellite images of sea surface temperature for each summer survey: 8 August 1998, 5 July 1999, 12 July 2000, 9 July 2002 and 5 July 2003. A cloud mask (white pixels) has been applied to all but the first image. Gray dots show location of CTD stations on NH and CR lines.

formalin/seawater. Samples were subsequently diluted and subsampled as described by Peterson and Keister (2002). Copepod densities were converted to biomass estimates using dry-weight/developmental-stage values found in the literature (e.g., Uye, 1982; Chisholm and Roff, 1990).

Upper-ocean currents were measured along each section by a shipborne acoustic Doppler current profiler (ADCP). On most cruises the ADCP system was narrowband, 153 kHz, 8-m bins, manufactured by RD Instruments. ADCP data were collected in 2.5 min ensembles and processed using the University of Hawaii CODAS system (Firing *et al*., 1995). Profiles were screened manually for bottom interference, corrected for gyrocompass errors with data from an Ashtech 3DF GPS-based system, calibrated for transducer and gyrocompass alignment, and processed to absolute currents by referring to differential GPS data. Kosro (2002) estimates high-frequency noise (due to tides and inertial currents) to be about ± 8 cm s^{-1}. The nominal depth of the shallowest useful bin was 25 m on all cruises. The processed ADCP data were interpolated to a standard grid with a horizontal resolution of 5 km (0 to 160 km offshore) and a vertical resolution of 5 m (25 to 150 m deep).

3. Results

a. Vertical distributions

The upper-ocean distributions (surface to 150 m depth) of selected parameters (temperature, salinity, nitrate and chlorophyll) are shown in Figure 5; distributions of additional parameters (density anomaly, spiciness, water velocity, phosphate, etc.) are included in a data report by Fleischbein *et al*. (2005).

Summer surface waters tend to be warmer off Newport, though subsurface waters tend to be cooler there than off Crescent City (Fig. 5a). Surface temperatures offshore of the shelf-break off Newport are remarkably uniform at 15–17°C, and very similar in different years. Offshore surface temperatures off Crescent City are much less homogeneous and exhibit greater variability.

Summer surface salinities tend to be lower off Newport than off Crescent City (Fig. 5b). The very fresh layer ($S < 32.5$ psu) off Newport is part of the Columbia River plume (Barnes *et al*., 1972; Cissell, 1969; Pak *et al*., 1970). Although the plume has a natural tendency to turn right as it exits the estuary at 46.25N (Hickey *et al.*, 1998), it is advected offshore and southward in summer by surface Ekman transport and the seasonal coastal jet (Barnes *et al.*, 1972; García Berdeal *et al.*, 2002). The plume entrains underlying seawater while *en route*: off Newport, the minimum surface salinity is usually about 30 psu and the base of the plume lies at a depth of 10–30 m.

Subsurface salinities are slightly lower off Newport than off Crescent City (Fig. 5b). At both locations there is a strong permanent halocline ($32.8 < S < 33.8$ psu) that has an offshore depth of 100 m and rises to intersect the sea surface inshore. This halocline is a permanent and ubiquitous feature of the Subarctic Pacific Ocean (Tully and Barber, 1960; Dodimead *et al.*, 1963; Tabata, 1976). Off Newport, this permanent halocline underlies the

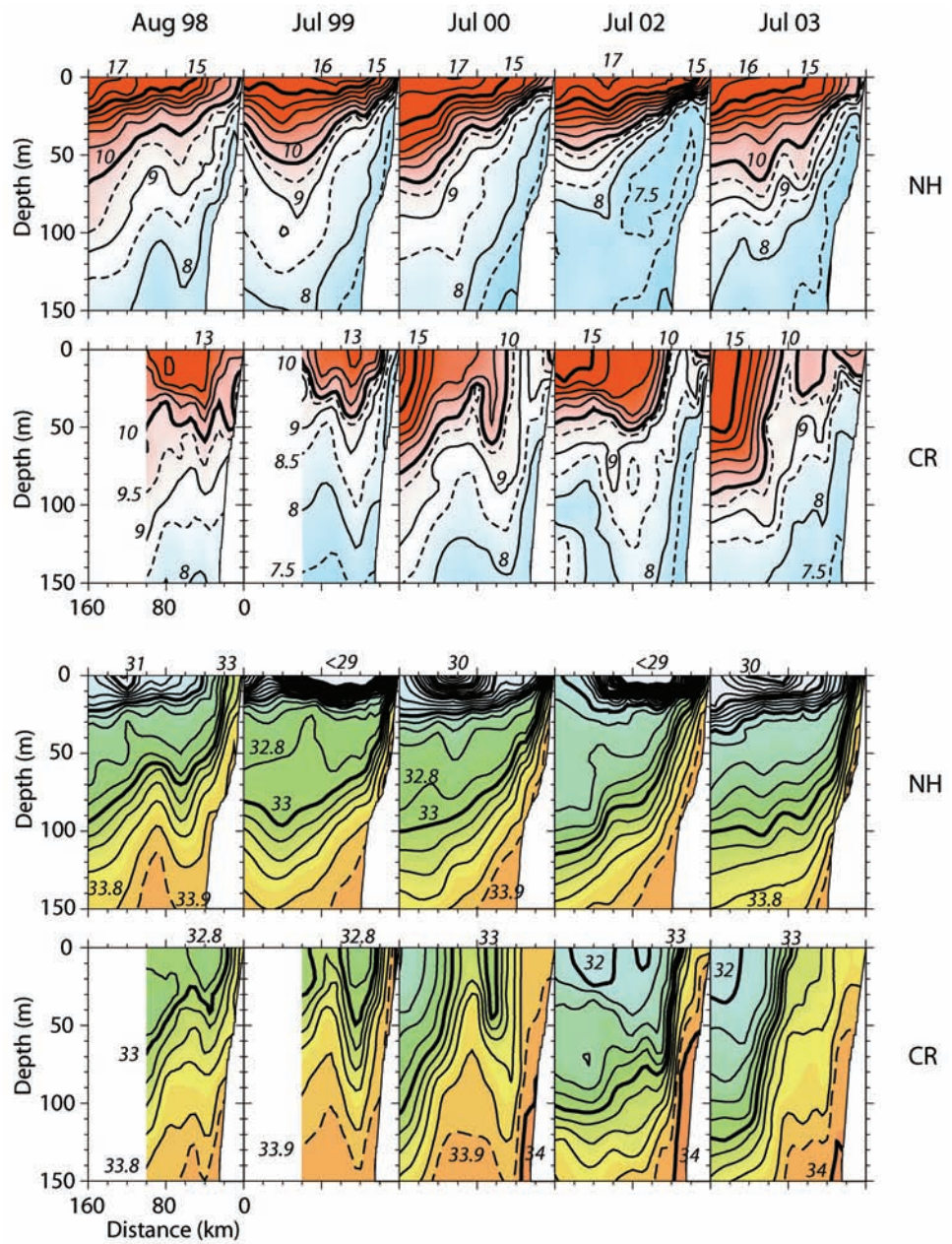

Figure 5. (a, b). Upper-ocean distributions of (a, *top*) temperature (°C) and (b, *bottom*) salinity (psu).

sharper seasonal halocline associated with the Columbia River plume. In both locations, the permanent halocline coincides with a permanent pycnocline with density anomaly (σ_t) range of 25.5 to 26.0 kg m^{-3}.

The combined T-S characteristics suggest several distinct water masses are present: the warm, fresh Columbia River plume waters (S $<$ 32.5 psu) off Newport; Subarctic water (32.5 $<$ S $<$ 33.8 psu; Tibby, 1941) in and above the permanent halocline which tends to be colder and fresher off Newport than off Crescent City; and deeper Subtropical water (S $>$33.9 psu, T $<$ 7 C, $\sigma_t > 26.5$ kg m^{-3}) which is only slightly fresher and cooler off Newport than off Crescent City. Wheeler *et al.* (2003) have suggested that most of the water that upwells is from the layer of Subarctic water. Occasionally, the 33.9 psu isohaline which marks the top of the deeper Subtropical layer is uplifted to depths as shallow as 30 m.

Nitrate concentrations (Fig. 5c) are depleted offshore in the surface layer off Newport, and there is no evidence that the Columbia River plume supplies any nitrates to this region (Hill and Wheeler, 2002). Nitrate concentrations in the upper 50 m tend to be much higher off Crescent City than off Newport, and the band of recently upwelled surface water (T $<$ 10°C and nitrates $>$ 5 μM) is much wider off Crescent City than off Newport. The distributions of other macro-nutrients (phosphate and silicate) are similar to the nitrate distributions (Fleischbein *et al.*, 2005).

Distributions of chlorophyll are quite different in the two locations (Fig. 5d). Off Newport, an inshore strong surface chlorophyll peak merges with a subsurface chlorophyll maximum that lies between the base of the Columbia River plume and the 5 μM nitrate isopleth. Although peak chlorophyll values off Crescent City also occur at the surface inshore, there is no continuous subsurface chlorophyll layer offshore: instead, we see isolated patches of moderately high concentrations of chlorophyll both within the surface layer and at depths greater than 50 m. The existence of these deep chlorophyll pockets is confirmed by fluorescence data (available for all five years), and by the dissolved oxygen data (available for four years; Fleischbein *et al*., 2005).

b. Significant differences

Summer mean values of selected physical, chemical and biological parameters were calculated for each line. For each parameter, the mean value at each location was obtained by simply averaging the individual observations made at the same location in five different years (August 1998, July 1999, July 2000, July 2002, July 2003). The standard error of the mean was estimated as the ratio of the population standard deviation (σ) to the square root of the number of samples, i.e., usually $\sigma/\sqrt{5}$. To compare values along the two sections, we have plotted mean values as a function of distance from shore; error bars represent plus/minus one standard error of the mean. We find that many features of the physical environment are significantly different in the two domains.

i. Surface salinity. The surface layer is significantly fresher off Newport than off Crescent City (Fig. 6a). Off Crescent City, the lowest salinity occurs at the offshore end of the section and has a value of about 32.1 psu, about 0.5 psu fresher than typical North Pacific Subarctic surface water; salinity increases monotonically toward shore, as we would expect if coastal upwelling were the only determining factor. Offshore surface salinities off

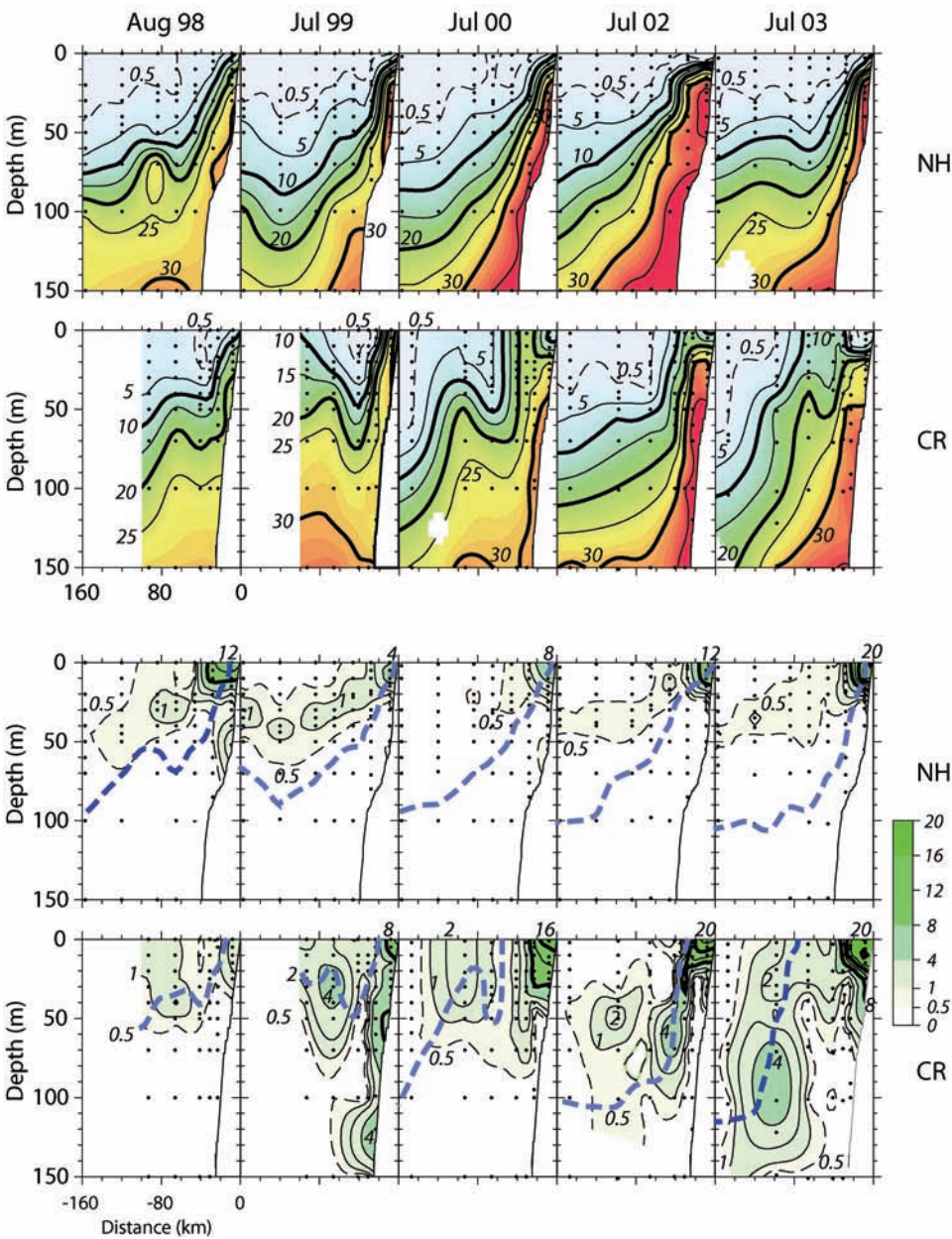

Figure 5. (c,d). Upper-ocean distributions of (c, *top*) nitrate (μM), top, and (d, *bottom*) chlorophyll (grams m^{-3}) with the 25.5 kg m^{-3} isopycnal surface (dashed blue line) superimposed.

Newport are lower (31 psu), and minimum values there (about 29 psu) occur in a band about 30–90 km from shore, defining the axis of the Columbia River Plume which is advected offshore by the Ekman transport and southward by the coastal jet in summer.

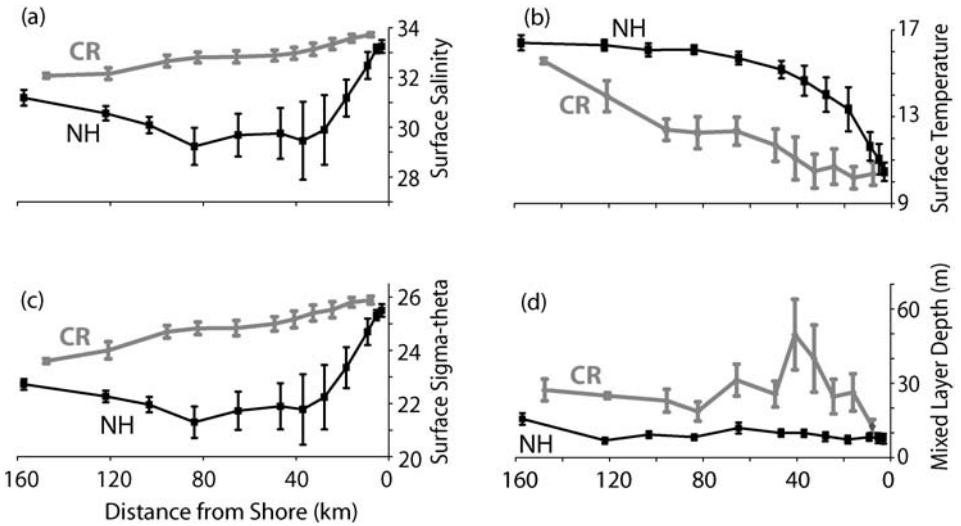

Figure 6. Zonal profiles of the means (±1 standard error) of (a) surface salinity, (b) surface temperature, (c) surface density, and (d) surface mixed layer depth as defined by a difference of 0.1 kg m^{-3} from the surface density.

ii. Surface temperature. The surface layer over the continental slope and outer shelf is significantly warmer off Newport than off Crescent City by about 3.5°C (Fig. 6b). Nelson and Husby (1983) suggest that the mean July net surface heat flux is about 230 W m^{-2} off both Newport and Crescent City. Thus the observed temperature differences are not likely the result of local heating, but must instead be due to dynamical processes including mixing, upwelling, and advection.

iii. Surface density. The combination of higher temperatures and lower salinities off Newport results in large surface density differences over the outer shelf and slope (Fig. 6c). The surface salinity difference of 3 psu (Fig. 6a) contributes about 2.5 kg m^{-3}, and the surface temperature difference of 3.5°C (Fig. 6b) contributes a further 0.6 kg m^{-3} to this density difference.

iv. Surface mixed layer depth. The reduced surface salinities off Newport contribute to enhanced stratification which tends to suppress vertical mixing by the wind. Distributions of the Brunt-Vaisala frequency as a function of depth and distance from shore (Fleischbein *et al.*, 2005) confirm the surface layer has very strong stratification off Newport, and much weaker stratification off Crescent City. Surface mixed layer depth can be defined in terms of a critical density gradient or in terms of a finite density change from the surface density (Brainerd and Gregg, 1995). To avoid aliasing due to the diurnal cycle of heating and cooling, we use a lax definition of "mixed layer depth" as the depth at which the seawater density exceeds surface density by 0.1 kg m^{-3}. Using this definition, we find the surface

Table 1. Light compensation depth, mixed layer depth, vertically integrated (0 to 150 m) biomass parameters, and mean ratios of particulate organic carbon to particulate organic nitrogen and to chlorophyll, for stations along the NH and CR lines. Entries for layer depths and integrated quantities show mean ±1 standard error.

Station name	Offshore dist. (km)	Comp. depth (m)	MLD (m)	Integrated chlor (mg m^{-2})	Integrated POC (mg m^{-2})	Integrated PON (mg m^{-2})	Mean POC/PON (mol/mol)	Mean POC/Chl (ug/ug)
NH5	9	18	8 ± 2	200 ± 61	14.6 ± 2.1	2.4 ± 0.5	8.58	230
CR1	8	14	13 ± 3	310 ± 86	13.4 ± 2.7	2.5 ± 0.5	6.46	62
NH15	28	28	9 ± 2	76 ± 31	16.9 ± 3.2	2.4 ± 0.4	7.73	310
CR3	24	15	25 ± 7	318 ± 85	20.4 ± 3.4	3.5 ± 0.7	7.24	184
NH25	47	31	10 ± 2	42 ± 4	15.6 ± 4.0	2.5 ± 0.8	7.64	324
CR5	41	22	50 ± 14	144 ± 54	13.8 ± 0.7	2.3 ± 0.3	8.18	155
NH35	65	32	12 ± 2	39 ± 5	12.7 ± 2.4	2.1 ± 0.5	7.59	328
CR7	66	22	31 ± 6	135 ± 45	16.9 ± 2.4	2.7 ± 0.3	7.46	177
NH45	84	31	8 ± 1	41 ± 6	11.7 ± 1.6	1.8 ± 0.4	7.56	271
CR9	95	19	23 ± 5	199 ± 79	18.0 ± 2.8	3.5 ± 0.6	6.40	160
NH65	122	33	7 ± 1	35 ± 6	10.2 ± 1.7	1.7 ± 0.3	7.59	349
NH85	157	33	16 ± 2	34 ± 6	8.0 ± 1.8	1.4 ± 0.1	8.11	346
CR11	148	34	27 ± 4	31 ± 6	11.4 ± 1.6	2.2 ± 0.4	6.43	464

layer depth to be significantly thinner off Newport than off Crescent City except over the inner shelf (Fig. 6d).

If the mixed-layer depth is large relative to the depth that photosynthetically-available radiation (PAR) penetrates the water column, phytoplankton photosynthesis could be light-limited. PAR data from selected stations sampled during daylight hours were used to calculate the extinction coefficient (k, with units m^{-1}) for light penetration through the water column. Most of the light attenuation is due to phytoplankton biomass and a linear regression of k versus integrated chlorophyll ($r^2 = 0.723$) provided an equation to calculate the extinction coefficient for all stations where we had integrated chlorophyll but not PAR data. Mean surface light intensity during the month of July is 35 quanta m^{-2} d^{-1} (Wetz and Wheeler, 2004) which is equivalent to a mean of 984 μmol quanta m^{-2} s^{-1} for a 14 h daylight period. We used the mean surface light intensity and the calculated extinction coefficients to determine the compensation depth (depth where PAR = 8 μmol quanta m^{-2} s^{-1}) for phytoplankton photosynthesis (Table 1). It is noteworthy that the light compensation depth is greater along the Newport line than the Crescent City line and that the compensation depth is greater than the mixed layer depth along the Newport line, but usually less than the mixed layer depth along the Crescent City line (Table 1). These results indicate that phytoplankton photosynthesis is likely to be light limited at Crescent City due to higher phytoplankton biomass, higher extinction coefficients, and deeper mixing of the surface layer.

v. Frontal position. As is clear from the satellite images (Fig. 4), the temperature front lies much farther from shore off Crescent City than off Newport. The location of the strongest

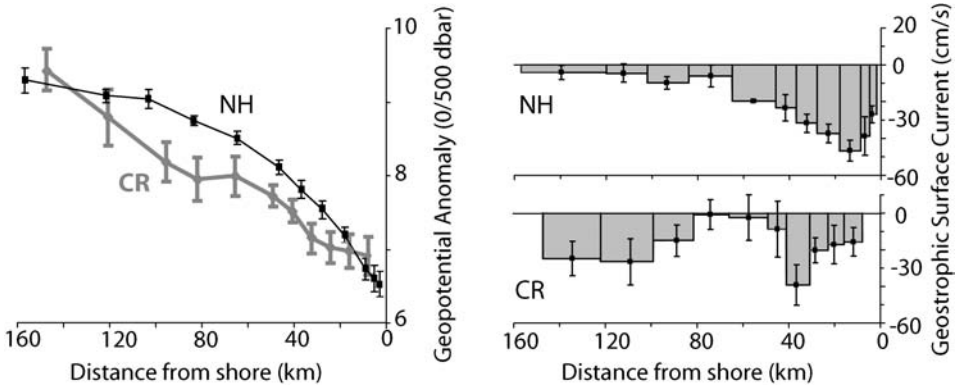

Figure 7. Zonal profiles of (a) mean surface elevation (geopotential anomaly relative to 500 dbar, J kg^{-1}), and (b) mean geostrophic surface current relative to 500 dbar. A geopotential anomaly of 1 J kg^{-1} corresponds to an elevation anomaly of 10 cm.

offshore gradient in average surface temperature (Fig. 6b) lies over the continental shelf off Newport (within 30 km of the coast), but much farther from shore (at about 120 km) off Crescent City. The band of cool surface water ($T < 13°C$) is only 20 km wide off Newport, but 100 km wide off Crescent City (Fig. 5a, 6b). Similarly the band of high surface salinity ($S > 32.5$ psu) is only 10 km wide off Newport, but 100 km wide off Crescent City. This combination confirms that the coastal upwelling front lies much farther offshore off Crescent City than at Newport.

vi. Surface elevation and geostrophic flow. Sea-surface elevation can be estimated from steric height, which is defined as the geopotential anomaly between the sea surface and a reference isobar; a steric height anomaly of 1.0 J kg^{-1} corresponds to an elevation anomaly of 10 cm. We calculated steric heights relative to the 500 dbar isobaric surface using the extrapolation procedure (see Appendix) described by Reid and Mantyla (1976) for each individual section, and then calculated means and standard errors (Fig. 7a). Over the outer shelf and slope, the sea surface is about 5 cm higher off Newport than off Crescent City, but inshore values and offshore values are about the same at the two locations. The error bars show that surface elevation is much more variable (by a factor of >2) off Crescent City than off Newport, suggesting stronger eddies or meanders there.

The geostrophic surface current (Fig. 7b) is directly proportional to the slope of the sea surface, southward (northward) where the surface slopes down (up) toward the coast. In the Appendix, we compare values of the geostrophic current computed from extrapolated steric heights with directly measured currents over the mid-shelf and find good agreement. Off Newport, the southward coastal jet is strongest over the mid-shelf, about 15 km from shore. Off Crescent City, the southward surface current has two separate cores: the core of a narrow inshore jet lies near the shelf-break, about 40 km offshore, and the core of a wider jet lies about 110 km from shore. Between them lies a band of weak and highly variable flow that may be associated with a recurring or persistent eddy over the continental slope.

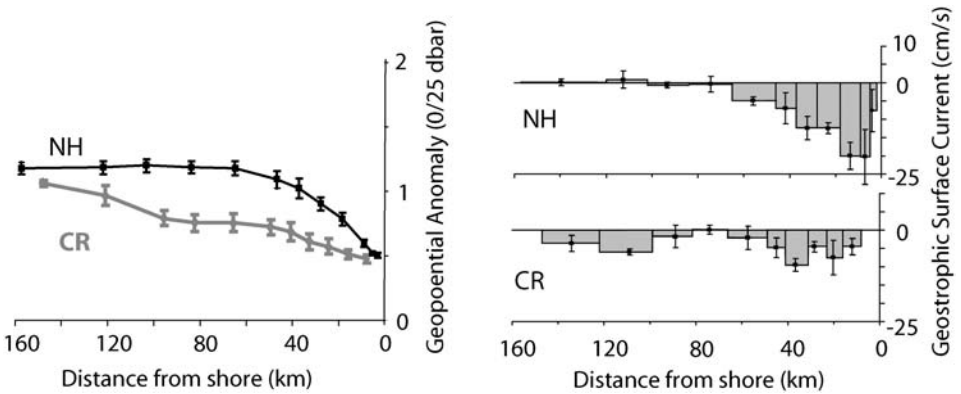

Figure 8. Zonal profiles of (a) mean surface elevation (geopotential anomaly relative to 25 dbar, J/kg), and (b) mean geostrophic surface current relative to 25 dbar.

A significant fraction of the geostrophic surface current is due to density gradients in the upper 25 m, particularly true off Newport, but also off Crescent City. Profiles of steric height and surface geostrophic flow (Fig. 8) relative to the 25 dbar isobar (which was sampled at all stations) show the vertical shear in this 25 m surface layer amounts to a single strong (20 cm s^{-1}) coastal jet off Newport, and weaker bimodal southward flow off Crescent City.

vii. Measured current. The alongshore (North-South) component of the ADCP current measured at 25 m shows a 60-km-wide southward current centered over the shelf-break 40 km off Newport, and a much stronger southward current centered 125 km offshore off Crescent City (Fig. 9a). Current reversals suggestive of eddies lie offshore of the southward jet off Newport, and inshore of the main core of the southward jet off Crescent City. A weak secondary southward jet lies near the shelf-break off Crescent City (about 30 km offshore). Southward flow in the jets penetrated to 150 m (Fig. 10) on both the NH line (core at 50 km offshore) and the CR line (core at 120 km). Along both sections, the most inshore measurements at 150 m show poleward flow along the shelf-break, but stronger and extending much farther out to sea off Crescent City (100 km from shore) than off Newport (40 km from shore). These features of the poleward flow were also observed in a large-scale survey in July-August 1995 (Pierce *et al*., 2000).

Combining the measured currents at 25 m (Fig. 9a) with the geostrophic current relative to 25 m (Fig. 8b) allows us to estimate the actual mean surface current (Fig. 9b). Comparison of the Newport and Crescent City profiles confirms that the main axis of the coastal jet lies nearshore (over the continental shelf) off Newport, but much farther out to sea off Crescent City.

viii. Surface nutrients and chlorophyll. Off Newport, high nutrient concentrations in the surface layer occur inshore of the mid-shelf (Fig. 11). Off Crescent City, high nutrient

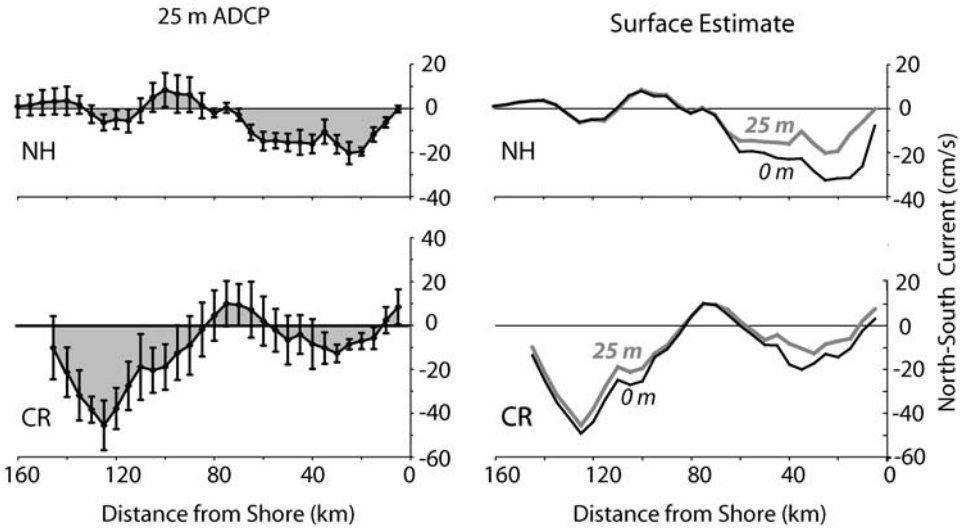

Figure 9. Zonal profiles of (a, *left*) the mean gridded alongshore (N-S) component of the ADCP-measured current at a depths of 25, and (b, *right*) estimate of the mean surface current obtained by adding the mean geostrophic surface current relative to 25 m to the mean ADCP current measured at 25 m.

concentrations occur over the entire shelf and slope, and even farther offshore. Offshore surface water along both lines is often very low in nitrate (< 0.5 μM) and these low concentrations are limiting to phytoplankton growth, especially for coastal diatoms (Corwith and Wheeler, 2002; Moses and Wheeler, 2003). Surface chlorophyll concentrations are similar off Newport and Crescent City, but high values of chlorophyll extend much deeper off Crescent City than they do off Newport (Fig. 5d). Values of vertically integrated chlorophyll are 3–4 times higher off Crescent City (Fig. 11). High chlorophyll concentrations at depths below the euphotic zone (50–60 m) off Crescent City are confirmed by the CTD fluorescence data (Fleischbein *et al*., 2005); these are also below the base of the surface mixed layer, and indicate that subduction may be more frequent off Crescent City than off Newport.

The mean chlorophyll level in the subsurface maximum off Newport is 0.93 ± 0.31 mg m^{-3}, while off Crescent City the mean for the years when the subsurface maxima are observed (1999, 2002, and 2003, Fig. 5d) is 4.77 ± 0.56 mg m^{-3}. Although the concentrations of particulate organic carbon (POC) and Chl are positively correlated for both transect lines, the ratio of POC:Chl (μg C/μg Chl) differs dramatically between the two sites, with a mean ($\pm$ std error) value of 308 ± 16 for the CR line and 194 ± 47 for the NH line (Table 1). The much lower POC:Chl ratios in the subsurface chlorophyll maximum off Crescent City are most likely due to light limitation at depth and a consequent increase in chlorophyll per cell as a photoadaptative response.

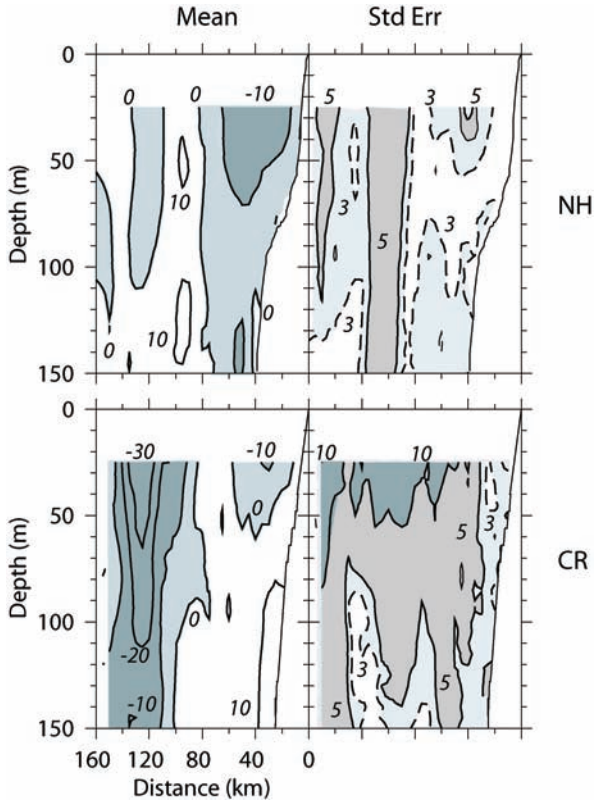

Figure 10. Vertical distributions of the mean and standard error of the alongshore component of the ADCP measured current. Southward mean flow is shaded.

ix. Copepod biomass. Peak copepod biomass occurred over the continental shelf off both Newport and Crescent City (Fig. 11). A second peak in biomass occurred offshore of Crescent City that was not seen off Newport; the offshore biomass peak corresponds in position to increased chlorophyll values (Fig. 11). The overall average copepod biomass was similar in the two domains (9.2 $\pm$ 2.5 mg C m^{-3} for the NH line and 9.5 $\pm$ 2.7 mg C m^{-3} for the CR line). Average biomass along each section varied substantially from year to year, ranging from 6 to 15 mg C m^{-3} off Newport, and from 4 to 14 mg C m^{-3} off Crescent City. Within cruises, average biomass was sometimes higher off Newport (1998 and 2000) and sometimes higher off Crescent City (1999, 2002, 2003).

4. Discussion

These significant differences have two major physical causes. The first is the spatial variation of the southward winds, and the second is advection of fresh water from the north. Both factors affect stratification and circulation in the region, and hence the supply of nutrients and plankton biomass.

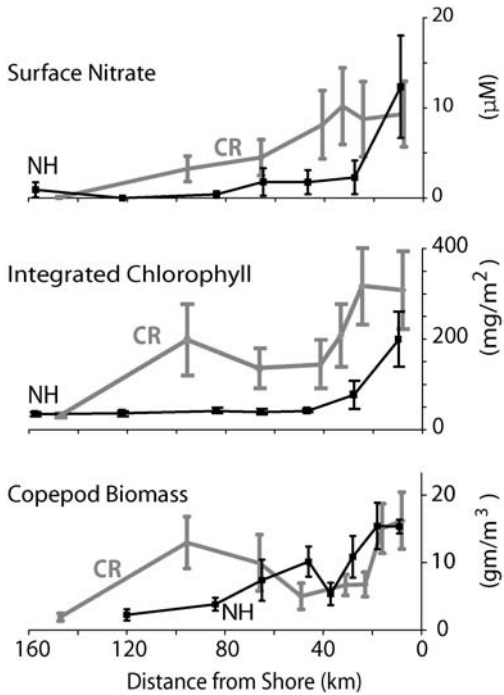

Figure 11. Zonal profiles of (a, *top*) mean surface nitrate (μM), (b, *middle*) mean vertically integrated chlorophyll (gm m^{-2}), and (c, *bottom*) mean copepod biomass in the upper 100 m.

a. Wind forcing

Surface winds affect the underlying upper ocean by three important processes (Gargett, 1991): mixing of the surface layer, coastal upwelling (or downwelling) nearshore due to offshore Ekman transport away from a solid boundary, and offshore upwelling (or downwelling) due to Ekman pumping resulting from divergence (or convergence) of Ekman transport due to an inhomogeneous wind field. The amount of energy available for mixing the surface layer is proportional to the cube of the wind speed (Husby and Nelson, 1982). Coastal upwelling carries deeper water into the coastal surface layer in an amount that balances the offshore Ekman transport ($M_E = \tau_c/f$, where τ_c is the alongshore component of the wind stress, and f is the local Coriolis parameter); this vertical transport occurs very near the coast (Lentz, 1994). At offshore locations, the vertical velocity at the base of the surface layer induced by Ekman pumping is proportional to the curl of the wind stress ($w_D = \text{curl}\ \boldsymbol{\tau}/(\rho f) = (\partial\tau_y/\partial x - \partial\tau_x/\partial y)/(\rho f)$, where $\boldsymbol{\tau}$ is the wind stress vector, τ_x and τ_y are its eastward and northward components, and ρ is the water density).

High resolution estimates of the wind stress in this region can be obtained from the SeaWinds scatterometer onboard the NASA QuikSCAT satellite launched in July 1999 (Samelson *et al.*, 2002; Perlin *et al.*, 2004). The QuikSCAT orbit provides twice-daily coverage at about 0300 UTC and 1400 UTC; summer observations are available for four

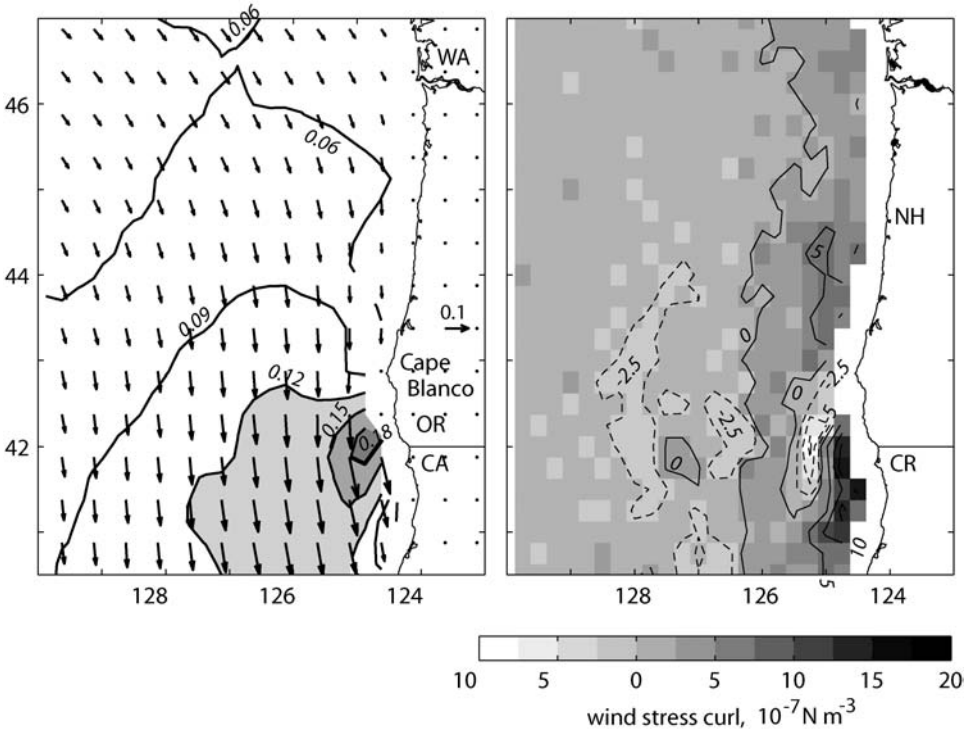

Figure 12. QuikSCAT mean July wind stress (*left,* a) and wind stress curl (*right,* b), 2000–2003. (a) Wind stress vectors and vector magnitudes (N m^{-2}). Every second vector of the 0.25° grid is shown. Mean values are computed only at grid points with 70 or more observations. (b) Curl of the mean July wind stress (10^{-7} N m^{-3}). First-order differencing caused the curl grid to be shifted 0.125° from the QuikSCAT grid, and the coastal data gap to widen. Positive (solid) contours are 5, 10, 15; negative (dashed) contours are −2.5, −5, −7.5. The 0 and −2.5 contours are shown only for larger features, ignoring small-scale oscillations.

years (2000–2003); results are interpolated onto a 0.25° grid (≈ 25 km). Contamination from land often results in an inshore gap of 30 km, and the number of observations in a given period drops steeply for the few last inshore grid points. The QuikSCAT mean July wind stress (Fig. 12a) has a southward component due to the persistent summer pressure gradient between the east Pacific high and the continental thermal low (e.g., Huyer, 1983; Kalnay *et al.*, 1996). The magnitude of the wind stress increases generally from north to south in our region; typical magnitudes are about twice as large off Crescent City (0.12 N m^{-2}) as off Newport (0.06 N m^{-2}, Fig. 12a; Nelson, 1977). This implies about three times more energy available for mixing the surface layer off Crescent City than off Newport; thus the large-scale variation in wind stress is a significant factor in explaining the deeper mixed layers on the CR line (Fig. 6).

The mean July wind stress magnitude is greatest in a tongue tending southwestward downwind of Cape Blanco (Fig. 12a). The wind stress intensification in the vicinity of

Cape Blanco is due to combined effects from a smaller-scale feature downwind of a cape and from a larger-scale bend in the Oregon-California coastline (Edwards *et al.*, 2001; 2002). Perlin *et al.* (2004) have shown that the local intensification is associated with an expansion fan due to the orographic effect in the inversion-topped marine atmospheric boundary layer on the leeward side of Cape Blanco. The local intensification may be an important mechanism for explaining the maximum in mixed layer depth that is observed 40 km offshore on the CR line (Fig. 6d). The wind maximum downwind of Cape Blanco also causes the local alongshore wind stress to be 3–4 times greater at 42N than at 44.5N (Fig. 12a). Consequently, the offshore Ekman transport and local coastal upwelling are 3–4 times greater off Crescent City than off Newport. This stronger coastal upwelling off Crescent City contributes to the very steep ascent of isotherms and other isopleths on the CR line (see Fig. 5a,b,c) and to the low temperatures and high nutrient concentrations observed there (Figs. 6, 11).

The July mean wind stress curl field (Fig. 12b) was derived by first-order central differencing of the QuikSCAT wind stress estimates. Positive and negative values of curl correspond to areas of local upwelling and downwelling, respectively. The region off central and northern Oregon is characterized by weak positive curl inshore, and weak negative curl offshore of about 126W. South of Cape Blanco, however, there is strong positive curl inshore of 125W (maximum $> 23 \cdot 10^{-7}$ N m^{-3}), strong negative curl between 125 and 125.5W (minimum $< -9 \cdot 10^{-7}$ N m^{-3}), and weak positive curl between 125.5 and 126W. The tongue of negative curl approaches Cape Blanco, thus interrupting the otherwise continuous band of positive wind stress curl adjacent to the coast. The tongue of intense negative mean curl coincides closely with the location of clockwise (anti-cyclonic) eddies or meanders observed southwest of Cape Blanco in August 1994 and August 1995 (Barth and Smith, 1998; Barth *et al.*, 2000). Variability of the July curl is also greatest in the region south and southwest of Cape Blanco: each of the first two empirical orthogonal functions (not shown) exhibits a strong dipole pair near 42N, 125W.

Zonal profiles of wind stress and wind stress curl along 44.5N (near the NH line) and along 42N and 41.5N (near the CR line) are compared in Figure 13. The first of these represents the domain north of Cape Blanco. The others represent the region affected by the orographically-perturbed flow in the marine atmospheric boundary layer: 42N contains the stress maximum; 41.5N contains the strongest curl. Off Newport, the southward wind stress varies only slightly, from -0.07 N m^{-2} offshore to -0.04 N m^{-2} inshore, and the curl is weakly negative offshore of 126W and positive inshore of 125.5W. Off Crescent City, the southward wind stress increases from -0.1 N m^{-2} offshore of 129W to -0.18 N m^{-2} at 125W; the curl is patchy but weak offshore of 126W, strongly negative between 125.5 and 125W, and strongly positive closer to shore. From these QuikSCAT data, we can estimate the relative importance of strictly coastal upwelling and offshore upwelling due to Ekman pumping. We follow the general methods of Pickett and Paduan (2003) who used wind stress estimates from large-scale atmospheric models to study these processes in the California Current system as a whole. Specifically, we compare vertical velocities at the base of the mixed layer at inshore (w_E) and offshore locations (w_D). The

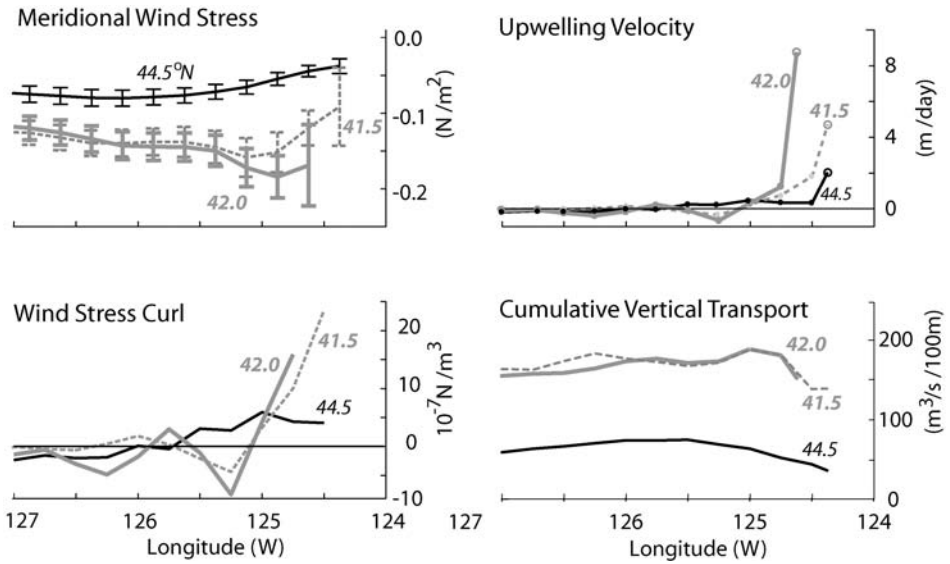

Figure 13. Zonal profiles of (a, *upper left*) meridional wind stress, (b, *lower left*) wind stress curl, (c, *upper right*) vertical velocity at the base of the ocean surface layer, and (d, *lower right*) cumulative vertical transport integrated westward from the coast, all at three latitudes: 44.5N near Newport, and 42.0N and 41.5N, both near Crescent City. Open circles in upper right panel represent w_E due to strictly coastal upwelling and small dots represent w_D due to Ekman pumping by the curl of the wind stress. For all of these profiles, mean values were computed at grid points with 45 or more observations; error bars in upper left panel represent 95% confidence intervals.

former can be estimated from $w_E = M_E/(\rho\,\lambda)$, where λ is the width of the coastal region in which the cross-shelf divergence occurs. In practice, we use the meridional wind stress data from the most inshore QuikSCAT grid point and, following Allen (1980, p. 391), a value of 15 km for λ to estimate w_E (open circles in Fig. 13c). Estimates of Ekman pumping velocity at offshore locations (w_D, defined above) are shown as small dots in Figure 13c. On all three zonal sections, the coastal upwelling (w_E) is much stronger than the offshore upwelling (w_D), and the coastal upwelling velocities are much stronger off Crescent City (9 m $^{-1}$ at 42N, 5 m d^{-1} at 41.5N) than off Newport (2.0 m d^{-1}). Ekman pumping is negligible off Newport, where the largest value of w_D is an order of magnitude smaller than the value of w_E . Off Crescent City, there is substantial upwelling over the outer shelf and upper slope ($w_D > 1$–1.5 m d^{-1} inshore of 125W, 65 km from shore) and appreciable downwelling between 125 and 125.5W ($w_D \approx -0.5$ m d^{-1}, 65–100 km from shore). The localized downwelling off Crescent City could be an important mechanism for generating the anticyclonic eddies observed on the CR Line (Fig. 6–8); it may also be an important mechanism for subducting high chlorophyll waters out of the surface layer.

Although the vertical velocities associated with Ekman pumping are generally small, the cumulative effect can be important (Fig. 13d). At 45N off Newport, the vertical transport due to coastal upwelling (due to wind stress at the most inshore grid-point) is 35 m^3 s^{-1} per

100 m of coastline, i.e., 0.35 $m^2\ s^{-1}$; including the Ekman pumping along the entire NH line (coast to 126W) increases the net vertical transport into the surface layer to 0.73 $m^2\ s^{-1}$. At 42N off Crescent City, the coastal upwelling contributes 1.52 $m^2\ s^{-1}$ while Ekman pumping adds 0.38 $m^2\ s^{-1}$ inshore of 125W but removes 0.16 $m^2\ s^{-1}$ between 125 and 126W.

Gan *et al*. (2005) have recently modeled the response of this coastal ocean to wind forcing from a regional atmospheric model. Samelson *et al*. (2002) showed that the atmospheric model wind stress fields generally resemble QuikSCAT fields (see their Figs. 2 and 5): both show much stronger alongshore wind stress at 42N than at 45 and 47N, though details of the gradients in the lee of Cape Blanco differ. The Gan *et al*. (2005) ocean model domain extends from 41.7N to 47.3N, and offshore 250 km from the coast. Their model was forced by wind stress and atmospheric heat flux from 1 June to 14 August 1999; it was initialized with zero velocities and horizontally uniform temperature and salinity profiles on 1 June; the first 15 days are regarded as spin-up. The 60-day average alongshore currents on their cross-shelf sections at 44.6N and 41.7N (in their Fig. 7) can be compared with our observations along the NH and CR lines. The model jet off Newport, like our NH line observations (Figs. 7–10), is strong ($\sim$50 cm s^{-1} at the surface), shallow (20 cm s^{-1} at 60 m), and nearshore (core at mid-shelf, 14 km from shore); both the model jet and our observations are consistent with coastal radar observations of shelf surface currents near Newport (Kosro, 2005). The model jet at 41.7N near Crescent City is stronger ($\sim$70 cm s^{-1} at the surface) and much deeper (30 cm s^{-1} at 180 m); in these respects it resembles the jet we observed on the CR line. However, the axis of the model jet at 41.7N lies near the shelf-break at the surface and tilts offshore with depth over the upper slope (30–50 km from shore), while the main core of the observed jet on the CR line lies much farther from shore (about 120 km; Figs. 9, 10). We speculate that this difference between model and observations may be due to the horizontally-uniform initial conditions in the model – especially since our observations show much stronger stratification off Newport than off Crescent City. But it is also possible that this difference is due to seasonal evolution of the coastal jet: Barth *et al*. (2005, their Fig. 7) show that the axis of the jet off Crescent City moved about 80 km offshore in two months, from the shelf-break in early June to 120 km offshore in early August 2000; seasonal processes are not adequately represented in the regional ocean model.

b. Fresh water advection

The prevailing southward currents in this region carry substantial amounts of low-salinity water, both from the Subarctic Pacific Ocean and from the Columbia River. Discharge from the Columbia River peaks in early summer (Sherwood *et al.*, 1990) when the discharge plume extends southwestward from its mouth at 46.25N. The NH line lies only 130 km south of the mouth, but the CR line lies about 400 km south of the mouth. The summer discharge is advected slowly offshore by Ekman transport and rapidly southward by the coastal jet.

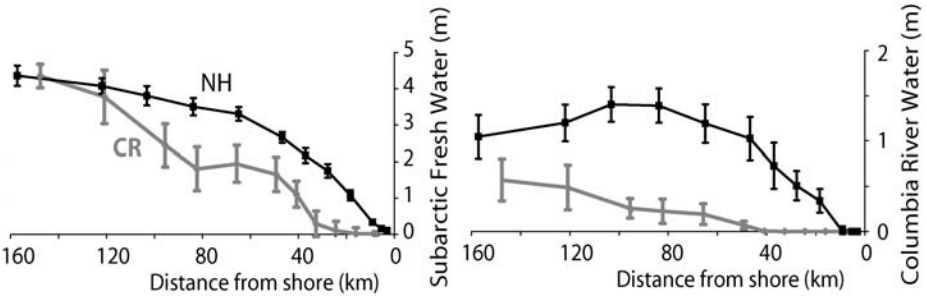

Figure 14. Estimates of the amounts of fresh water advected from the Subarctic Pacific Ocean (*left*), and from the Columbia River (*right*). Note that vertical scales differ.

The equivalent depth of the amount of fresh water at a given location can be estimated by vertically integrating the observed salinity profile (Tully and Barber, 1960):

$$F_S = (S^*L - \int_0^L Sdz)/S^*$$

where S is the measured salinity, S^* is the value of the reference salinity, L is the depth at which it occurs, and F_{S^*} is the equivalent depth of fresh water (in meters) above the reference salinity. Historical studies suggest reference values of 33.8 and 32.5 psu for the Subarctic Pacific and the Columbia River Plume, respectively (Tully and Barber, 1960; Barnes *et al.*, 1972). In our region, integrating down from the sea surface to 33.8 psu would include fresh water from the Columbia (F_{CR}) as well as fresh water from the Subarctic (F_{SA}); we therefore estimate the purely Subarctic fraction as the difference between $F_{33.8}$ and $F_{32.5}$. Figure 14 shows that the Subarctic contribution is similar on the offshore portions of the NH and CR lines ($F_{SA} = 4$ m), decreasing to zero at the coast due to upwelling (more rapidly on the CR line). Figure 14 also shows that the contribution from the Columbia River is much larger on most of the NH line ($F_{CR} = 1.4$ m at 90 km) than on the CR line ($F_{CR} = 0.5$ m offshore), i.e., the NH line intersects the plume, while the CR line extends only to the inshore flank of the plume.

As noted by Barnes *et al.* (1972), the influence of the Columbia River discharge in this region is an inherently seasonal phenomenon. This is consistent with our observations: early spring sections (March or April, 1998–2003) show much less Columbia River water on the NH-line ($F_{CR} \approx 0.5$ m), and almost no water fresher than 32.5 psu on the CR line. River discharge increases during the spring season (Sherwood *et al.*, 1990), and the alongshore coastal jet (Barth *et al.*, 2005) carries fresh plume waters southward, first past Newport and later past Crescent City; remnants have been observed as far south as 39N off Pt Arena, California later in summer (Kosro and Huyer, 1986; Huyer *et al.*, 1998). In our summer sections along the NH and CR line, the core of the plume lies on the offshore side of the baroclinic jet. Although the Columbia River plume is thin, it contains a substantial

fraction of the total fresh water in this region, and it is an important factor in accounting for higher stratification, a thinner mixed layer and warmer surface temperatures off Newport.

c. Biological processes, physical forcing and carbon export

Deeper mixing and stronger upwelling off Crescent City than off Newport results in an increased nutrient supply and higher standing stocks of chlorophyll in surface waters off Crescent City. The deep pockets of chlorophyll off Crescent City are below the euphotic zone and at least in 2003 are distinct (separate) from the surface chlorophyll maximum. The particulate material is characterized by low carbon-to-nitrate (C:N) ratios and very low carbon-to-chlorophyll (C:Chl) ratios suggesting that this is recently subducted material. Temperature-salinity and oxygen-salinity characteristics of the CR line data (shown in Fleischbein *et al.*, 2005) are also consistent with subduction. During both 2002 and 2003 the chlorophyll pockets lie along the 33 psu isohaline and 25.6 isopycnal (Fig. 4b, d). Similar deep chlorophyll maxima were observed farther south in the California Current by Barth *et al.* (2002). Off California the main subsurface chlorophyll maximum was observed at 150–200 depth with chlorophyll concentrations of 1–2 mg m^{-3}. The main feature was attributed to downwelling along sloping density surfaces through the conservation of potential vorticity along the meandering jet path. The weaker subsurface chlorophyll maximum was attributed to sinking phytoplankton in a cyclonic eddy. In both 2002 and 2003, the deep chlorophyll observed off Crescent City lay near the main core of the coastal jet, which was closer to shore in July 2002 than in July 2003.

The subsurface chlorophyll maximum off Newport is continuous with the surface maximum and could result from phytoplankton sinking as surface water is advected offshore or from downward flux along an isopycnal. However, it is also consistent with local production in a regime with an upwarped nutricline. Surface water is depleted in nitrate and the subsurface chlorophyll maximum is located at depths where nitrate ranges from 1–5 μM. This is much lower than the > 15 μM nitrate levels in the deep chlorophyll pockets off Crescent City. Wherever nitrate is < 0.5 μM within the mixed layer the phytoplankton are likely to be nitrogen limited. As shown in Figure 4c, the spatial extent of the low nitrate mixed layer water is much greater off Newport than off Crescent City. Thus, offshore of Newport the phytoplankton are more likely to be nutrient limited. Deeper mixing off Crescent City results in higher nutrient concentrations but also results in exposure of phytoplankton to lower irradiances. The observation that the mixed layer depth exceeds the compensation depth for net photosynthesis and the low POC/Chl ratio off Crescent City both suggest that the phytoplankton are likely to be light limited there. Potential export of particulate organic carbon off Newport can be estimated as the mean integrated POC from 40 to 160 km offshore as 11.6 ± 1.2 mg POC m^{-2} (mean ± SE). In contrast the potential export of particulate organic carbon of Crescent City over the same distance is 15.6 mg POC m^{-2} (mean ± SE). The stronger upwelling, stronger mixing, and the offshore position of the jet off Crescent City result in higher nutrient inputs to surface water, higher phytoplankton standing stocks and a doubling of potential cross-shelf export of particulate carbon.

The offshore peak in mean copepod biomass seen off Crescent City but not off Newport was likely a result of stronger upwelling and the formation of the offshore core of the jet in the region south of Cape Blanco. The strong upwelling-favorable winds there drive both the upwelling front and the coastal jet much farther offshore than in the northern region off Newport. The offshore peak in the mean copepod biomass results from high biomass at the 95 km station in 1999, 2000, and to a lesser extent 2003. Those were all years in which satellite images (Fig. 4) and our temperature sections (Fig. 5a) showed cold, recently-upwelled surface water extending offshore to the 95 km station. In 2002, the front lay nearer shore (Figs. 4, 5a), and offshore copepod biomass values were all characteristic of warm-water stations. Surface nitrate values at the 95 km station ranged from 1–2 μM during 1999, 2000 and 2003, compared to < 0.5 μM other years off Crescent City and all years off Newport. Integrated chlorophyll values at the 95 km CR station ranged from 141–508 mg chl m^{-2} during 1999, 2000 and 2003, compared to 67–123 mg chl m^{-2} other years off Crescent City and a mean of 41 ± 12 mg chl m^{-2} all years at the 84 km station off Newport. Thus, there appear to be very clear links between increased winds and upwelling with colder temperatures, higher nutrients, higher phytoplankton standing stocks, and higher copepod biomass.

5. Conclusions

We find important summer-season differences in the coastal upwelling domains north and south of Cape Blanco at 42.9N. Compared to the domain off Newport (44.6N), the domain off Crescent City (41.9N) has a more saline, cooler, denser and thicker surface mixed layer; a wider coastal zone inshore of the upwelling front and jet; a strong offshore core as well as a weak inshore core of the southward surface current; higher nutrient concentrations in the photic zone; and higher phytoplankton biomass. Copepod biomass was high over the shelf in both locations; copepod biomass was also high in the offshore core of the coastal jet off Crescent City. The CR line shows evidence of deep chlorophyll pockets that have been subducted from the surface layer; no such pockets were observed off Newport. Phytoplankton biomass tends to be nutrient-limited off Newport, and light-limited off Crescent City. We attribute these differences to stronger mean northerly wind stress over the southern domain, to strong small-scale wind stress curl in the lee of Cape Blanco, and to reduced influence of the Columbia River discharge in the coastal region south of Cape Blanco. These strong differences between two adjacent domains in the northern California Current provide the physical basis for the biogeographical boundary at Cape Blanco (Parrish *et al.*, 1981) and also show that we must be cautious in extrapolating results from only local studies to regional or global ecosystems.

Acknowledgments. We are grateful to Michael Freilich and Dudley Chelton for providing the QuikSCAT satellite wind data; to Ted Strub for providing the satellite sea-surface temperature data; to John Allen and Roger Samelson for frequent discussions; and to anonymous reviewers for important comments. Huyer, Fleischbein, Kosro, Smith, and Wheeler were supported by the National Science Foundation (Grants OCE-0000733 and OCE-0434810); Perlin was supported by the National Science Foundation (OCE-9907854) and by the Office of Naval Research (Grant N00014-

01-0231); and Keister was supported by the National Oceanic and Atmospheric Administration (Grants NA86OP0589, NA17FE275 and NA17RJ1372). This is contribution number 251 of the U. S. GLOBEC program, jointly funded by the National Science Foundation and the National Oceanic and Atmospheric Administration.

APPENDIX

The credibility of extrapolated geostrophic currents

Reid and Mantyla (1976) demonstrated that the elevation of the sea surface measured by coastal tide gages agrees with the steric height (geopotential anomaly). Their results depend on a procedure for extrapolating steric heights relative to a deep reference level into the shallow waters of the inner shelf. The procedure assumes that there is no lateral shear at the depth of the deepest sample of a CTD station over the upper slope or shelf. This assumption allows one to calculate the geopotential anomaly at the maximum depth of a CTD station shallower than the reference level by simple linear extrapolation from its two nearest offshore neighbors. Working stepwise from offshore provides the geopotential anomalies and geostrophic currents even over the shelf.

In an unpublished poster paper (Smith *et al.*, 2000), we compared the geostrophic current estimated from extrapolated steric height with moored current meter and shipborne ADCP observations made during GLOBEC LTOP. In this Appendix we present a comparison of the extrapolated geostrophic currents (V_g) at a mid-shelf location on the NH line with the currents (V_{ADCP}) from the shipborne ADCP during 16 NH-line sections made between September 1997 and September 2000, and with the currents (V_{ADP}) measured by moored Acoustic Doppler Profiler. To provide a larger range of oceanographic conditions, late summer (September), fall, winter and spring sections are included in the comparison as well as summer data discussed in this paper.

Geopotential anomalies relative to 500 db were calculated from the CTD observations along the NH line (which extended east-west, nearly normal to the coastline) using the Reid and Mantyla extrapolation method. The north-south (alongshore) component of geostrophic velocity (V_g) was calculated by simple differencing of geopotential anomalies from the adjacent stations, NH-10 and NH-15, 18 and 28 km off the coast, in water 80 and 90 m deep, respectively. The NH line surveys included the continuous operation of a shipborne 153 kHz Acoustic Doppler Current Profiler. The ADCP velocities were binned in 8 m intervals centered at 25 m, 33 m, etc. The ship-borne ADCP data were averaged horizontally from NH-10 to NH-15 for the purposes of comparison with the geostrophic currents. Figure 15 (dashed line, x) shows the north-south component of ADCP velocity (V_{ADCP}) at 33 m for 16 cross-margin sections, compared with the geostrophic current (V_g) at 30 m. A bottom-mounted Acoustic Doppler Profiler, moored slightly south and offshore of NH-10, provided continuous current measurements for most of the water column (10–65 m) during most of the GLOBEC LTOP study period. The north-south ADP currents at the time of the CTD observations were taken from 40-hr low-passed ADP time series. Figure 15 (solid line, dots) shows the north-south component of ADP velocity (V_{ADP}) at 30 m compared with the geostrophic current (V_g) for 14 cross-margin sections.

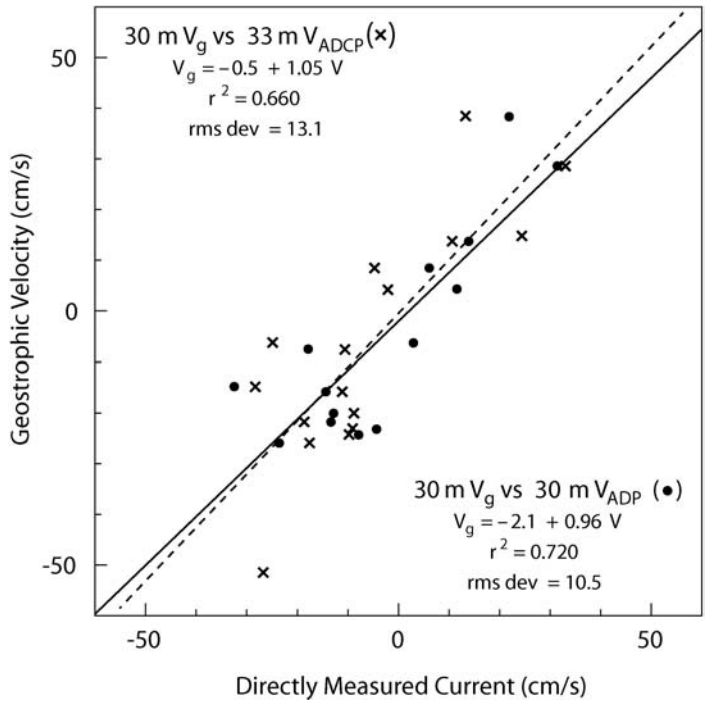

Figure 15. Comparison of mid-shelf geostrophic currents with low-passed alongshore currents measured at the NH-10 ADP mooring (dots) and alongshore currents measured by the ship-borne ADCP between NH-10 and NH-15 (crosses). Results of linear regression are shown as solid line (for ADP mooring) and dashed line (for ship-borne ADCP) and in the legends.

The comparisons between mid-shelf geostrophic velocities show good agreement with measured currents, with regression slopes close to 1 and intercepts close to 0. The RMS deviations of mid-shelf extrapolated geostrophic currents from measured currents are about 10 cm s^{-1}, much smaller than the seasonal range of the alongshore current but about the same magnitude as day-to-week variations in summer.

REFERENCES

Allen, J. S. 1980. Models of wind driven currents on the continental shelf. Ann. Rev. Fluid Mech., *12,* 389–433.

Bakun, A. 1973. Coastal upwelling indices, West Coast of North America, 1946–71. U. S. Dept of Commerce, NOAA Tech. Rep. NMFS SSRF-671, Seattle, 114 pp.

Barnes, C. A., A. C. Duxbury and B.-A. Morse. 1972. Circulation and selected properties of the Columbia River effluent at sea, *in* The Columbia River Estuary and Adjacent Ocean Waters, Bioenvironmental Studies, A. T. Pruter and D. L. Alverson, eds., University of Washington Press, Seattle, 41–80.

Barth, J. A., T. J. Cowles, P. M. Kosro, R. K. Shearman, A. Huyer and R. L. Smith. 2002. Injection of carbon from the shelf to offshore beneath the euphotic zone in the California Current. J. Geophys. Res., *107,* doi: 10.1029/2001JC000956.

Barth, J. A., S. D. Pierce and T. J. Cowles. 2005. Mesoscale structure and its seasonal evolution in the northern California Current System. Deep-Sea Res. II, *52,* 5–28.

Barth, J. A., S. D. Pierce and R. L. Smith. 2000. A separating coastal upwelling jet at Cape Blanco, Oregon and its connection to the California Current System. Deep-Sea Res. II, *47,* 783–810.

Barth, J. A. and R. L. Smith. 1998. Separation of a coastal upwelling jet at Cape Blanco, Oregon, USA. Benguela Dynamics. S. Afr. J. Mar. Sci., *19,* 5–14.

Brainerd, K. E. and M. C. Gregg. 1995. Surface mixed and mixing layer depths, Deep-Sea Res., *42,* 1521–1543.

Chisholm, L. A. and J. C. Roff. 1990. Size-weight relationships and biomass of tropical neritic copepods off Kingston, Jamaica. Mar. Biol., *106,* 71–77.

Cissell, M. C. 1969. Chemical Features of the Columbia River Plume off Oregon, M. S. Thesis, Dept. Oceanography, Oregon State University, Corvallis, Oregon, 45 pp.

Corwith, H. L. and P. A. Wheeler. 2002. El Niño related variations in nutrient and chlorophyll distributions off Oregon. Prog. Oceanogr., *54,* 361–380.

Dodimead, A. J., F. Favorite and T. Hirano. 1963. Salmon of the North Pacific Ocean – Part II. Review of oceanography of the Subarctic Pacific Region. Int. N. Pac. Fish. Comm. Bull., *13,* 195 pp.

Edwards, K. A., C. E. Dorman and D. P. Rogers. 2002. Adjustment of the marine atmosphere boundary layer to the large-scale bend in the California coast. J. Geophys. Res., *107,* 3213, doi:10.1029/2001JC000807.

Edwards, K. A., A. M. Rogerson, C. D. Winant and D. P. Rogers. 2001. Adjustment of the marine atmospheric boundary layer to a coastal cape. J. Atmos. Sci., *58,* 1511–1528.

Firing, E., J. Ranada and P. Caldwell. 1995. Processing ADCP data with the CODAS software system, version 3.1,University of Hawaii, Honolulu, HI.

Fleischbein, J., J. Hill, A. Huyer, R. L. Smith and P. A. Wheeler. 1999. Hydrographic data from the GLOBEC long-term observation program off Oregon, 1997 and 1998, College of Oceanic and Atmospheric Sciences, Oregon State University, Data Report *172,* Ref. *99-1,* 288 pp. (Available on http://ltop.coas.oregonstate.edu.)

Fleischbein, J., A. Huyer and R. L. Smith. 2001. Hydrographic data from the GLOBEC long-term observation program off Oregon, 1999 and 2000. College of Oceanic and Atmospheric Sciences, Oregon State University, Data Report *183,* Ref. *2001–3,* 290 pp. (Available on http://ltop.coas.oregonstate.edu.)

—— 2002. Hydrographic data from the GLOBEC long-term observation program off Oregon, 2001, College of Oceanic and Atmospheric Sciences, Oregon State University, Data Report *187,* Ref. *2002–3,* 168 pp. (Available on http://ltop.coas.oregonstate.edu.)

—— 2003. Hydrographic data from the GLOBEC long-term observation program off Oregon, 2002 and 2003, College of Oceanic and Atmospheric Sciences, Oregon State University, Data Report *192,* Ref. *2003-2,* 296 pp. (Available on http://ltop.coas.oregonstate. edu.)

Fleischbein, J., A. Huyer, R. L. Smith, and P. A. Wheeler. 2005. Upper ocean water properties and currents along paired sections in the northern California Current, summer 1998–2003, College of Oceanic and Atmospheric Sciences, Oregon State University, Data Report *201,* Ref. *2005-4,* 41 pp. (Available on http://ltop.coas.oregonstate.edu.)

Gan, J., J. S. Allen and R. M. Samelson. 2005. On open boundary conditions for a limited-area coastal model off Oregon. Part 2: response to wind forcing from a regional mesoscale atmospheric model. Ocean Model., *8,* 155–173.

García Berdeal, J., B. M. Hickey and M. Kawase. 2002. Influence of wind stress and ambient flow on a high discharge river plume. J. Geophys. Res., *107,* doi: 10.1029/2001JC000932.

Gargett. A. E. 1991. Physical processes and the maintenance of nutrient-rich euphotic zones. Limnol. Oceanogr., *36,* 1527–1545.

Halpern, D. 1976. Structure of a coastal upwelling event observed off Oregon during July 1973, Deep-Sea Res., *23,* 495–508.

Hickey, B. M., L. J. Pietrafesa, D. A. Jay and W. C. Boicourt. 1998. The Columbia River Plume study: Subtidal variability in the velocity and salinity fields. J. Geophys. Res., *103,* 10339–10368.

Hill, J. K. and P. A. Wheeler. 2002. Organic carbon and nitrogen in the northern California Current system during July 1997: comparison of offshore, river plume, and coastally upwelled water. Prog. Oceanogr., *53,* 369–387.

Husby, D. M. and C. S. Nelson. 1982. Turbulence and vertical stability in the California Current. CalCOFI Rep., *23,* 113–129.

Huyer, A. 1983. Coastal upwelling in the California current system. Prog. Oceanogr., *12,* 259–284.

Huyer, A., J. A. Barth, P. M. Kosro, R. K. Shearman and R. L. Smith. 1998. Upper-ocean water mass characteristics of the California Current, summer 1993. Deep-Sea Res. II, *45,* 1411–1442.

Huyer, A., R. L. Smith and J. Fleischbein. 2002. The coastal ocean off Oregon and Northern California during 1997–8 El Niño. Prog. Oceanogr., *54,* 311–341.

Kalnay, E., M. Kanamitsu, R. Kistler, W. Collins, D. Deaven, L. Gandin, M. Iredell, S. Saha, G. White, J. Woollen, Y. Zhu, M. Chelliah, W. Ebisuzaki, W. Higgins, J. Janowiak, K. C. Mo, C. Ropelewski, J. Wang, A. Leetmaa, R. Reynolds, R. Jenne and D. Joseph. 1996. The NCEP/NCAR 40-Year Reanalysis Project, Bull. Amer. Meteor. Soc., *77,* 437–431.

Kosro, P. M. 2002. A poleward jet and an equatorward undercurrent observed off Oregon and northern California during the 1997–98 El Niño. Prog. Oceanogr., *54,* 343–360.

—— 2005. On the spatial structure of coastal circulation off Newport, Oregon during spring and summer 2001, in a region of varying shelf width. J. Geophys. Res. (submitted).

Kosro, P. M. and A. Huyer. 1986. CTD and velocity surveys of seaward jets off northern California, July 1981 and 1982. J. Geophys. Res., *91,* 7680–7690.

Kundu, P. K. and J. S. Allen. 1976. Some three-dimensional characteristics of low-frequency current fluctuations near the Oregon coast. J. Phys. Oceanogr., *6,* 181–199.

Laurs, R. M. 1967. Coastal upwelling and the ecology of lower tropic levels. Ph. D. Thesis. Oregon State University, 121 pp.

Lentz, S. J. 1994. Current dynamics over the Northern California inner shelf. J. Phys. Oceanogr., *24,* 2461–2478.

Mooers, C. N. K, C. A. Collins and R. L. Smith. 1976. The dynamic structure of the frontal zone in the coastal upwelling region off Oregon. J. Phys. Oceanogr., *6,* 3–21.

Moses, W. C. and P. A. Wheeler. 2004. Seasonal and across-shelf trends of the phytoplankton community of the Oregon coastal environment, College of Ocean and Atmospheric Sciences, Oregon State University, Data Report *194,* Northeast Pacific GLOBEC Long-term Observation Program. (Available on http://ltop.coas.oregonstate.edu.)

Nelson, C. S. 1977. Wind stress and wind stress curl over the California Current. U.S. Dept. of Commerce., NOAA Tech. Rep. NMFS SSRF-714. 87 pp.

Nelson, C.S. and D. M. Husby. 1983. Climatology of surface heat fluxes over the California Current region. U.S. Dept. of Commerce., NOAA Tech. Rep. NMFS SSRF–763. 155 pp.

Pak, H., G. F. Beardsley, Jr. and P. K. Park. 1970. The Columbia River as a source of marine light scattering particles. J. Geophys. Res., *75,* 4570–4578.

Parrish, R. H., C. S. Nelson and A. Bakun. 1981. Transport mechanisms and reproductive success of fishes in the California Current, Biol. Oceanogr., *1,* 175–203.

Perlin, N., R. M. Samelson and D. B. Chelton. 2004. Scatterometer and model wind and wind stress in the Oregon – northern California coastal zone. Monthly Weather Rev., *132,* 2110–2129.

Peterson, W. T. and J. E. Keister. 2002. The effects of a large cape on distribution patterns of coastal and oceanic copepods off Oregon and northern California during the 1998–99 El Niño – La Niña. Prog. Oceanogr., *53,* 389–411.

Pickett, M. H. and J. D. Paduan. 2003. Ekman transport and pumping in the California Current based

on the U. S. Navy's high-resolution atmospheric model (COAMPS). J. Geophys. Res., *108,* doi: 10.1029/2003JC001902.

Pierce, S. D., R. L. Smith, P. M. Kosro, J. A. Barth and C. D. Wilson. 2000. Continuity of the poleward undercurrent along the eastern boundary of the mid-latitude North Pacific. Deep-Sea Res. II, *47,* 811–829.

Reid, J. L. and A. W. Mantyla. 1976. The effect of geostrophic flow upon coastal sea elevations in the northern North Pacific Ocean. J. Geophys. Res., *81,* 3100–3110.

Samelson, R. M., P. Barbour, J. Barth, S. Bielli, T. Boyd, D. Chelton, P. Kosro, M. Levine, E. Skyllingstad and J. Wilczak. 2002. Wind stress forcing of the Oregon coastal ocean during the 1999 upwelling season. J. Geophys. Res., *107,* doi: 10.1029/20001JC000900.

Sherwood, C. R., D. Jay, R. B. Harvey, P. Hamilton and C. A. Simenstad. 1990. Historical changes in the Columbia River estuary. Prog. Oceanogr., *25,* 299–352.

Small, L. F. and D. W. Menzies. 1981. Patterns of primary productivity and biomass in a coastal upwelling region. Deep-Sea Res., *28A,* 123–149.

Smith, R. L. 1981. A comparison of the structure and variability of the flow field in three coastal upwelling regions: Oregon, Northwest Africa, and Peru, *in* Coastal Upwelling, F.A. Richards, ed., Am. Geophys. Union, 107–118.

—— 1995. The physical processes of coastal upwelling systems, *in* Upwelling in the Ocean: Modern Processes and Ancient Records, C. P. Summerhayes, K.-C. Emeis, M. V. Angel, R. L. Smith and B. Zeitzschel, eds., John Wiley, 39–64.

Smith, R. L., A. Huyer and J. Fleischbein. 2001. The coastal ocean off Oregon from 1961 to 2000: Is there evidence of climate change or only of Los Niños? Prog. Oceanogr., *49,* 63–93.

Smith, R. L., A. Huyer and P. M. Kosro. 2000. The credibility of extrapolated geostrophic currents. EOS Trans. Am. Geophys. Union, *81(48),* Fall Meet. Suppl., Abstract OS71B-15. (Complete poster available on http://ltop.coas.oregonstate.edu).

Smith, R. L., J. G. Pattullo and R. K. Lane. 1966. An investigation of the early stage of upwelling along the Oregon coast. J. Geophys. Res., *71,* 1135–1140.

Tabata, S. 1976. The general circulation of the Pacific Ocean and a brief account of the oceanographic structure of the North Pacific Ocean, Part II - Thermal regime and influence on climate. Atmosphere, *14,* 1–27.

Tibby, R. B. 1941. The water masses off the west coast of North America. J. Mar. Res., *4,* 112–121.

Tully, J. P. and F. G. Barber. 1960. An estuarine analogy in the Subarctic Pacific Ocean. J. Fish. Res. Bd. Canada, *17,* 91–112.

Uye, S. 1982. Length-weight relationships of important zooplankton from the inland Sea of Japan. J. Ocean. Soc. Jap., *38,* 149–158.

Weitkamp, L., P. Busby and K. Neely. 1997. Geographical variation in life histories of salmonids, *in* Estuarine and Ocean Survival of Northeastern Pacific Salmon, R. L. Emmett and M. H. Schiewe, eds., U. S. Dept. Commerce, NOAA Tech. Mem. NMFS-NWFSC-29, 27–34.

Wetz, M. S., P. A. Wheeler and R. M. Letelier. 2004. Light-induced growth of phytoplankton collected during the winter from the benthic boundary layer off Oregon, USA. Mar. Ecol. Prog. Ser., *280,* 95–104.

Wheeler, P. A., A. Huyer and J. Fleischbein. 2003. Cold halocline, increased nutrients and higher chlorophyll off Oregon in 2002. Geophys. Res. Lett., *30,* doi:10.1029/2003GL017395.

Received: *10 February, 2005*; revised: *28 April,* 2005.